Article

Not peer-reviewed version

Cranial Investigations of Crested Porcupine (*Hystrix cristata*) by Magnetic Resonance Imaging and Anatomical Gross-sections

Daniel Morales Bordon , Mario Encinoso Quintana * , Alberto Arencibia , José Raduan Jaber *

Posted Date: 31 May 2023

doi: 10.20944/preprints202305.2165.v1

Keywords: Magnetic resonance imaging; gross sections; rodents; head anatomy; CNS; crested porcupine

Article

Cranial Investigations of Crested Porcupine (*Hystrix cristata*) by Magnetic Resonance Imaging and Anatomical Gross-sections

Daniel Morales Bordon [1], Mario Encinoso Quintana [2,*], Alberto Arencibia [3] and José Raduan Jaber [3,*]

[1] Departamento de Patología Animal, Producción animal, Bromatología y Tecnología de los alimentos, Facultad de Veterinaria, Universidad de Las Palmas de Gran Canaria, Trasmontaña, Arucas, 35413 Las Palmas, Spain; daniel.morales@ulpgc.es (D.M);
[2] Hospital Clínico Veterinario, Facultad de Veterinaria, Universidad de Las Palmas de Gran Canaria, Trasmontaña, Arucas, 35413 Las Palmas, Spain; mencinoso@gmail.com (M.E.)
[3] Departamento de Morfologia, Facultad de Veterinaria, Universidad de Las Palmas de Gran Canaria, Trasmontaña, Arucas, 35413 Las Palmas, Spain; alberto.arencibia@ulpgc.es (A.A); joseraduan.jaber@ulpgc.es (J.R.J)
* Correspondence: mencinoso@gmail.com (M.E.); joseraduan.jaber@ulpgc.es (J.R.J)

Simple Summary: Advanced imaging diagnostic techniques such as magnetic resonance imaging with anatomical gross sections were used to evaluate the head of the crested porcupine (*Hystrix cristata*). These techniques were very helpful to delineate the main formations that compose the central nervous system (CNS), as well as its associated structures. To the authors' knowledge, the present study is the first to describe this area by MRI and gross sections in crested porcupines.

Abstract: This paper aimed to describe an atlas of the head of the crested porcupine (*Hystrix cristata*), applying advanced imaging techniques such as MRI. Furthermore, by combining the images acquired through these techniques with anatomical gross sections, we obtained an adequate description of the structures that form the CNS and associated structures of this species. This anatomical information could serve as a valuable diagnostic tool for the clinical evaluation of different pathological processes in porcupines such as abscesses, skull malformations, fractures, and neoplasia.

Keywords: magnetic resonance imaging; gross sections; rodents; head anatomy; CNS; crested porcupine

1. Introduction

In recent years, advanced diagnostic imaging techniques have facilitated the visualization of several diseases in wildlife medicine. Traditionally, standard radiography was the choice more frequently used by clinicians [1]. Nevertheless, results of previous studies have demonstrated that computed tomography (CT) and magnetic resonance imaging (MRI) gives more information to improve diagnostic accuracy, prognosis, treatment of diseases, and anatomic knowledge [2-4]. These modern techniques avoid the superimposition of adjacent anatomical structures and delineate the anatomic detail of specific tissue densities more finely, which improves its interpretation [2]. These benefits provide important value for the anatomic investigations of specific regions, providing essential knowledge in domestic and exotic mammal species [2-5]. Among these species, we highlight the crested porcupine *(Hystrix cristata),* which is one of the most well-known members of the Family Hystricidae, and is included in the IUCN red list as least concern since they are regionally or locally threatened, mainly due to they are hunted illegally for food and killed because they are contemplated as an agricultural pest [6,7]. Consequently, these animals require appropriate conservation policies in regional and local contexts. It is a species of rodent native to Italy and Sicily and a broad central strip ranging from Senegal and west to Somalia and east to Kenya and Tanzania, but very little is

Preprints (www.preprints.org) | NOT PEER-REVIEWED | Posted: 31 May 2023 doi:10.20944/preprints202305.2165.v1

known regarding its geographic variability in Africa [6-8]. These animals are found in forests, rocky areas, mountains, croplands and sandhill deserts and protect in caves, aardvark holes and burrows that they dig themselves [6,7].

Porcupines are characterized for presenting strong and pointed quills covering their tail, sides and top of the body that can be raised into a crest and used for defensive purposes. Concerning its head, it is large and robust with an enlarged infraorbital foramen so that portions of the masseter extend through it and arise from the frontal side surface of the snout. Besides, the nasal cavity is enlarged [9]. Interestingly, Hystrik show prominent pockets in the skull, maxillary, lacrimal and turbinate bones, which could be used for attachment of the masticatory muscles

Some valuable literature on the anatomical, physiological and pathological study of pet rabbits and rodents is already broadly available [10-16]. Among these, we highlighted those studies that deal with brain and head MRI anatomy, which are available at reduced resolution from low field-strength and cross-sections, and more recently, with a high field-strength magnet in excised and fixed rabbit brain for research and clinical guide in animals with diverse pathological processes [14-15]. To the best of the authors' knowledge, only a few publications have been conducted on porcupines, focused on their biology, morphometric geographic variability and some clinical conditions such as upper respiratory tract disease [6,8,9,13]. However, no description of the brain has been reported in this specific rodent. Therefore, this study aimed to describe the normal anatomy of the CNS of the crested porcupine and its associated structures, using MRI and specific anatomic gross sections that better matched the images obtained by imaging techniques. The combination of MRI and macroscopic anatomical sections could provide helpful information for anatomic teaching and clinical practice.

2. Materials and Methods

2.1. Animals

Two carcasses of adult male crested porcupines (*Hystrix cristata),* from the zoological park "Rancho Texas Lanzarote Park" (Lanzarote, Canary Islands, Spain) were collected. None of the porcupines used in this study had a history of central nervous system disease, and no abnormalities were detected during imaging examinations.

2.2. Anatomic Evaluation

After the MR images were acquired, the two scanned carcasses were frozen at -80 ºC for 48 hours before performing anatomical-gross sections. After that, the two frozen carcasses were sectioned using an electric band saw to get sequential anatomical cross-sections. Contiguous 1 cm transverse slices were obtained starting at the olfactory bulb and extending to the first cervical vertebra region. These slices were intentionally thicker than those of the MRI to keep the integrity and position of the anatomic formations in the slices. The sections obtained were cleaned with water, numbered and photographed on the cranial and caudal surfaces. Later, we selected those anatomic sections that better correlated with the MRI images to identify the structures of the crested porcupine central nervous system and associated structures. Moreover, we also used anatomical textbooks and relevant references describing the anatomy of cats, rabbits and different rodent species to facilitate accurate anatomic identification of the CNS and associated structures [14,15,17,18,19,20,21].

2.3. MRI technique

The magnetic resonance imaging study of each crested porcupine was conducted with a 1.5-Tesla magnet (Toshiba, Vantage Elan, Japan) with the animal placed in ventral recumbence. A standard MRI protocol was used to generate spin-echo (SE) T1-weighted, and T2-weighted images in sagittal, transverse, and dorsal planes. SE T1-weighted transverse images were acquired with the following settings: Echo time (TE), 10 ms, repetition time (TR), 800 ms, acquisition matrix of 536 x 384, and 4.5 mm slice thickness with 4 mm spacing between slices. For SE T2-weighted transverse images, the TE 120 ms, TR 10541 ms, acquisition matrix 624 x 448, and 3 mm slice thickness with 3 mm interslice spacing. For SE T2-weighted sagittal images, the TE 120 ms, TR 7529 ms, acquisition matrix 512 x 804, and 2.8 mm slice thickness with 2 mm interslice spacing. For SE T2-weighted dorsal images, the TE 120 ms, TR 8282 ms, acquisition matrix 468 x 512, and 3.4 mm slice thickness with 3 mm interslice spacing. We used a medical imaging viewer (OsiriX MD, Geneva, Switzerland) to evaluate the images of the study.

3. Results

In this study, we present different anatomical gross sections and T2W images of the crested porcupine, which are displayed in a rostral to caudal progression from the level of the olfactory bulb and eyeballs to the caudal end of the brain stem. Therefore, figure 1 is a T2W sagittal image in which each line and number (I-V) represent approximately the level of the following anatomical and MRI transverse images. Transverse gross sections and MR images of the porcupine revealing the relevant anatomical structures of the head are displayed (Figures 2-6). These figures are composed of two images: A) Macroscopic gross-section. B) T2W MR image. Additionally, two sagittal and two dorsal T2W MR images are presented to depict the relevant structures of the porcupine central nervous system (Figures 7-8).

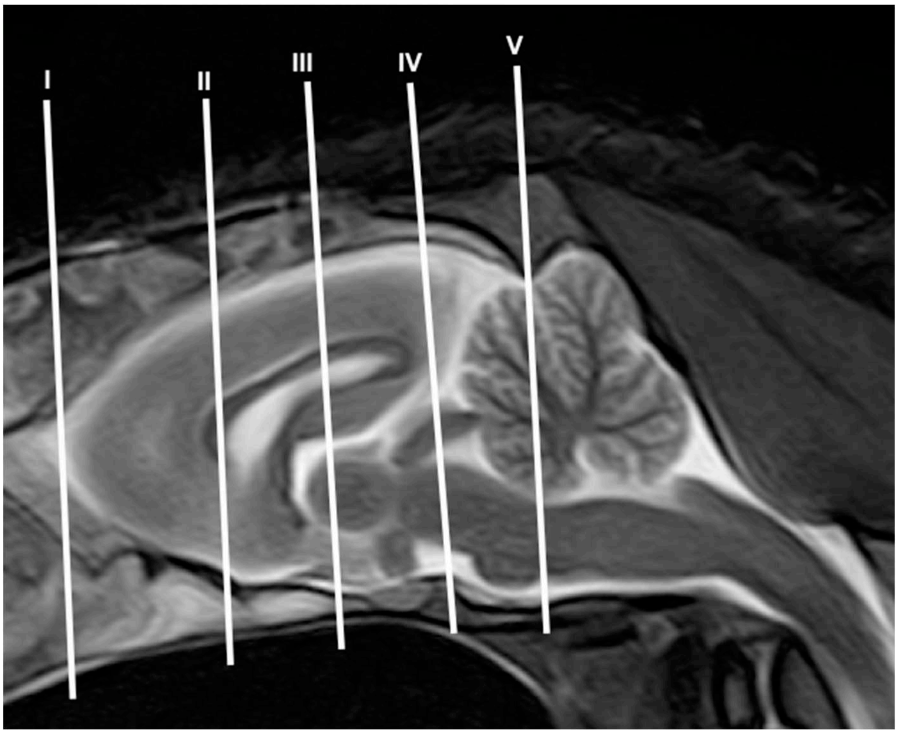

Figure 1. Sagital T2W MR image of the head of the crested porcupine. The lines and numbers (I–VI) represent the approximate level of the following transverse gross sections and MR images.

3.1. Anatomical gross-sections

Anatomical sections obtained in this study allowed us to visualize the different structures belonging to the central nervous system and its associated structures, which were labelled according to the International Committee on Veterinary Gross Anatomical Nomenclature. Therefore, we identified the main components of the brain (the prosencephalon, mesencephalon and rhombencephalon). Thus, the two telencephalic hemispheres surrounded by the cerebral cortex and separated by the longitudinal cerebral fissure could be identified (Figs. 4A, 5A, 6A). Both hemispheres were connected by fibres of white matter known as the corpus callosum (Figs. 3A, 4A, 5A, 6A). Each cerebral hemisphere contains a lateral ventricle (Figure 3A, 4A, 5A, 6A). Ventrally, we distinguish a component of the basal ganglia, the nucleus caudatus (Fig. 3A, 4A, 5A). Thus, we identify different parts of it such as the head and the tail (Figs. 3A, 4A, 5A). Other structures observed were the septal nuclei, which are circumscribed by two parallel vertical lines through the most

Preprints (www.preprints.org) | NOT PEER-REVIEWED | Posted: 31 May 2023 doi:10.20944/preprints202305.2165.v1

inferior and medial aspect of each lateral ventricle (Figure 3A). More caudally, the diencephalon (thalamus) enclosing the third ventricle was identified, and more ventrally specific components of the hypothalamus, such as the optic chiasm (Figs. 3A, 4A). Additionally, these sections were quite helpful to show the caudal part of the thalamus. Hence, the lateral eminence on the caudodorsal surface of the thalamus also known as the lateral geniculate body was distinguished, whereas caudoventrally, we identified the medial geniculate body of the thalamus (Fig. 5A). Moreover, the dorsal part of the mesencephalon with the caudal and rostral colliculus, and its ventral part with the cerebral peduncles were also shown (Fig. 6A). These sections were helpful identifying the vermis and the cerebellar peduncles, which connected the cerebellum to the adjacent brain stem and the cerebrum (Fig. 6A). The ventral part of the cerebellum with the nodule, covering part of the fourth ventricle could also be identified (Fig. 6A). These sections were also helpful distinguishing the medulla oblongata and the decussation of the pyramids. In addition, different bony structures that comprise the **neurocranium** were observed, such as the frontal, the temporal (with its scamous, and the petrous and tympanic parts), the sphenoid, and the occipital bones (Figs. 3A, 4A, 5A, 6A). Besides, these sections allowed the identification of different air-filled spaces such as the frontal and the sphenoidal sinuses (Figs. 2A, 3A, 4A, 5A, 6A). Besides, structures associated with the nasal cavity, such as the ethmoturbinates and the cartilage of the nasal septum could be distinguished (Figs. 2A, 3A, 4A, 5A, 6A). Main sensory organs such as the eyeball and associated structures were also depicted Therefore, we identify the retina, the vitreous chamber, and the optic nerve surrounded by extraocular muscles. Among these, we distinguished the dorsal and ventral rectus muscles (Fig. 2A). Moreover, the main components of the auditory system such as the external auditory canal, the tympanic cavity, and the inner ear were visualized (Figs. 4A, 5A). Also, we identified relevant muscles related to the masticatory function, such as the temporalis, the medial pterygoid muscles and the masseter, the digastric and other important muscles such as the buccinator muscle, and the longissimus capitis of the head (Figs. 2A, 3A, 4A, 5A, 6A).

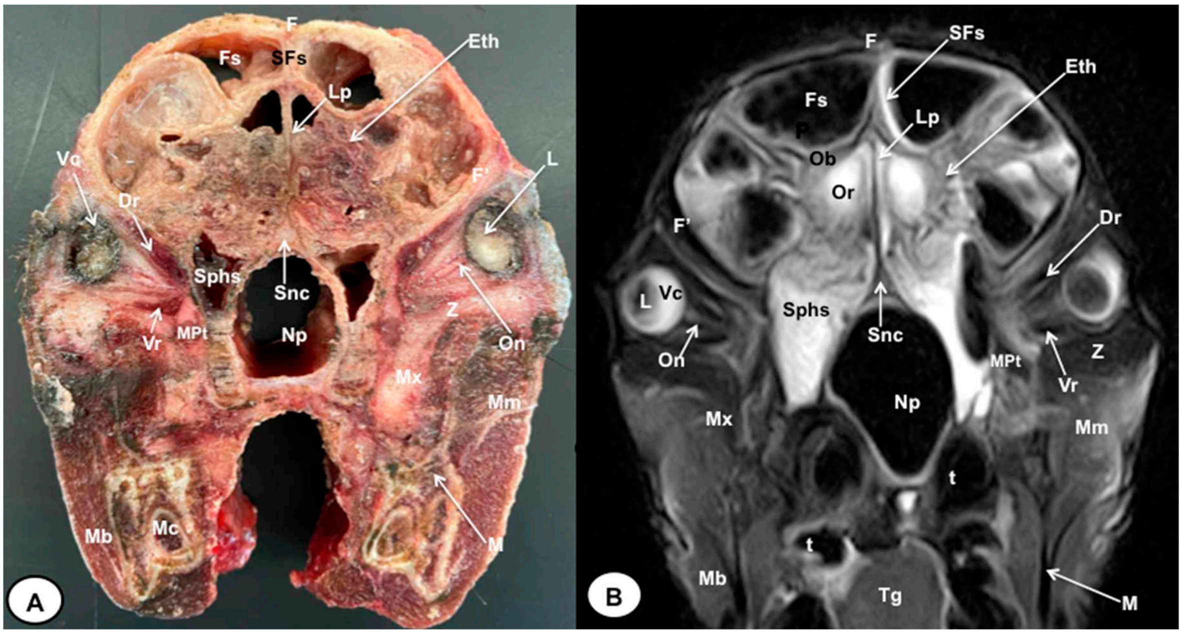

Figure 2. : Transverse gross-section (A) and T2W MR (B) images of the crested porcupine head. F: Frontal bone. F': Orbital plate of frontal bone Fs: Frontal sinuses. SFs: Septum of frontal sinuses. Eth: Ethmoturbinates. Ob: Olfactory bulb. Or: Olfactory recess. Lp: *Lamina perpendicularis ossis ethmoidei.* Sphs: Sphenoid sinus. Snc: Septal nasal cartilage. Np: Nasopharynx. On: Optic nerve. Vc: Vitreous chamber. L: Lens. Dr: *Musculus rectus dorsalis*. Vr: *Musculus rectus ventralis*. MPt: *Musculus pterygoideus medialis*. Z: Zygomatic bone. Mx: Maxillary bone. T: Tooth. M: Mandible. Mc: Mandibular canal. Mm: *Musculus masseter*. Mb: *Musculus buccinator*. Tg: Tongue.

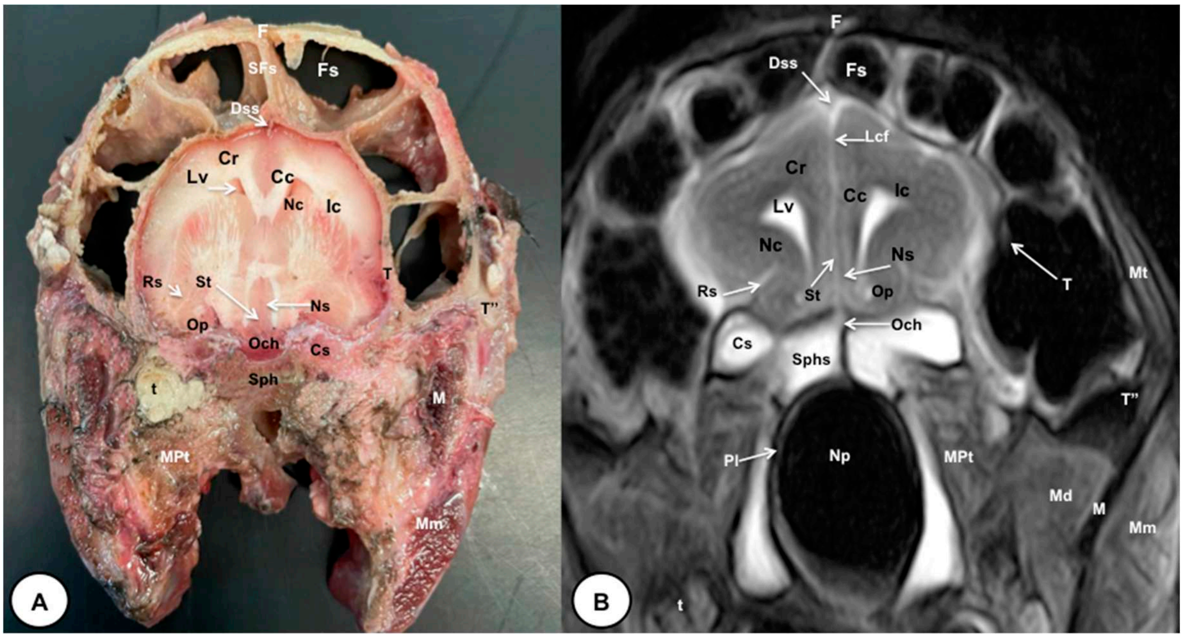

Figure 3. Transverse gross-section (A) and T2W MR (B) images of the crested porcupine head. F: Frontal bone. Fs: Frontal sinuses. SFs: Septum of frontal sinuses. Dss: Dorsal sagittal sinus. Lcf: Longitudinal cerebral fissure. Cc: Corpus callosus. Cr: *Corona radiata*. Lv: Lateral ventricle. *Nucleus caudatus*. Ic: Internal capsule. Rs: Rhinal sulcus. St: *Septum telencephali*. Ns: *Nuclei septi*. Op: Olfactory peduncle. Och: Optic chiasm. Cs: Cavernous sinus. T. Temporal bone (Squamous part). T'': Zygomatic process of temporal bone. Pl: Palatine bone (*Lamina perpendicularis*). Sph: Sphenoid bone. Sphs: Sphenoid sinus. Np: Nasopharynx. Mt: *Musculus temporalis*. MPt: *Musculus pterygoideus medialis*. Md: *Musculus digastricus* M: Mandible.. Mm: Musculus masseter. t: Tooth.

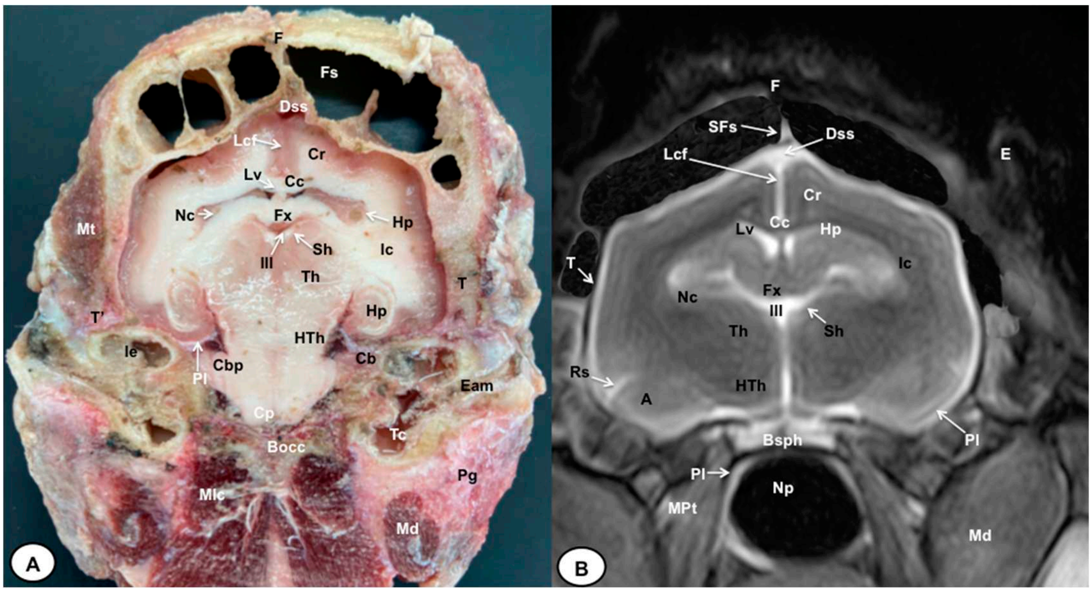

Figure 4. Transverse gross-section (A) and T2W MR (B) images of the crested porcupine head. F: Frontal bone. Fs: Frontal sinuses. SFs: Septum of frontal sinuses. Dss: Dorsal sagittal sinus. Lcf: Longitudinal cerebral fissure. Cc: Corpus callosus. Cr: *Corona radiata*. Lv: Lateral ventricle. Fx: Fornix. Hp: *Hippocampus*. Nc: *Nucleus caudatus*. Ic: Internal capsule. III: Third ventricle. Sh: *Stria habenularis*. Th: *Thalamus*. HTh: *Hypothalamus*. A: *Amygdala*. Pl: Piriform lobe. Cbp: Cerebellar peduncle. Cp: Cerebral peduncle. T: Temporal bone squama. T′: Tympanic and petrous parts of temporal bone. Pl: Palatine bone (*Lamina perpendicularis)*. Bsph: Basisphenoid bone. Bocc: Basioccipital bone. Np: Nasopharynx. MPt: *Musculus pterygoideus medialis*. Mlc: *Musculus longissimus capitis*. Md: *Musculus digastricus*. Pg: Parotid gland. Ie: Inner ear. Tc: Tympanic cavity. E: Ear (external part).

Preprints (www.preprints.org) | NOT PEER-REVIEWED | Posted: 31 May 2023 doi:10.20944/preprints202305.2165.v1

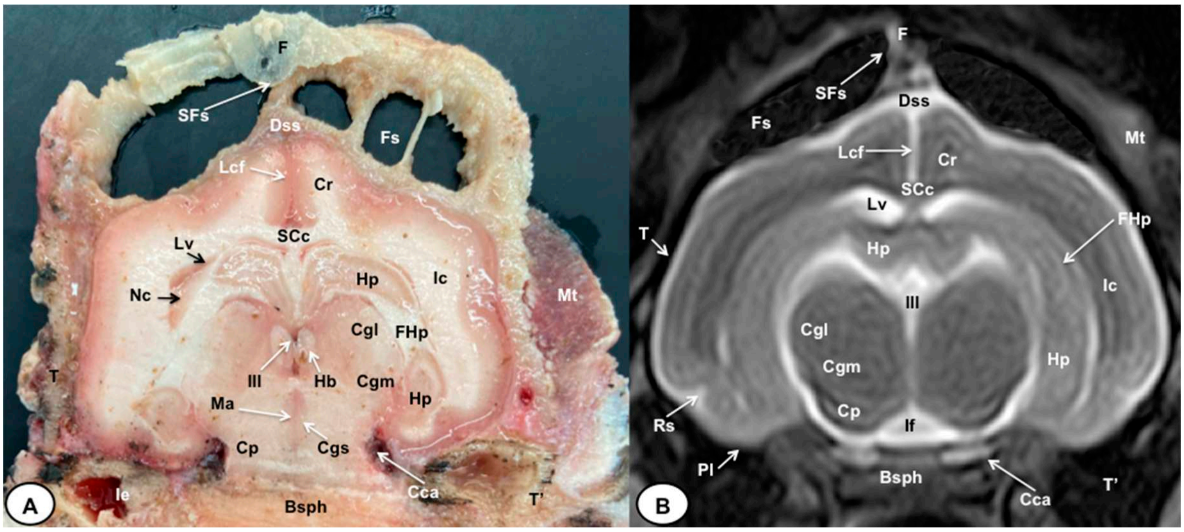

Figure 5. Transverse gross-section (A) and MRI in T2W (B) images of the crested porcupine head. F: Frontal bone. Fs: Frontal sinuses. SFs: Septum of frontal sinuses. Dss: Dorsal sagittal sinus. Lcf: Longitudinal cerebral fissure. SCc: Splenium of corpus callosum. Cr: *Corona radiata*. Lv: Lateral ventricle. Hp: *Hippocampus*. FHp. Fimbria of hippocampus. Nc: ***Nucleus caudatus*** **(**tail*)*. Ic: Internal capsule. III: Third ventricle. Hb: Habenula. Cgl: *Corpus geniculatum laterale* (lateral geniculate body). Cgm: *Corpus geniculatum mediale* (medial geniculate body). Ma: Mesencephalic aqueduct. Cgs. Central grey substance. Cp: Cerebral peduncle. If: Interpeduncular fossa. Rs: Rhinal sulcus. Pl: Piriform lobe. T: Temporal bone squama. T′: Tympanic and petrous parts of temporal bone. Ie: Inner ear. Cca: Caudal communicating artery. Bsph: Basisphenoid bone. Mt: *Musculus temporalis.*

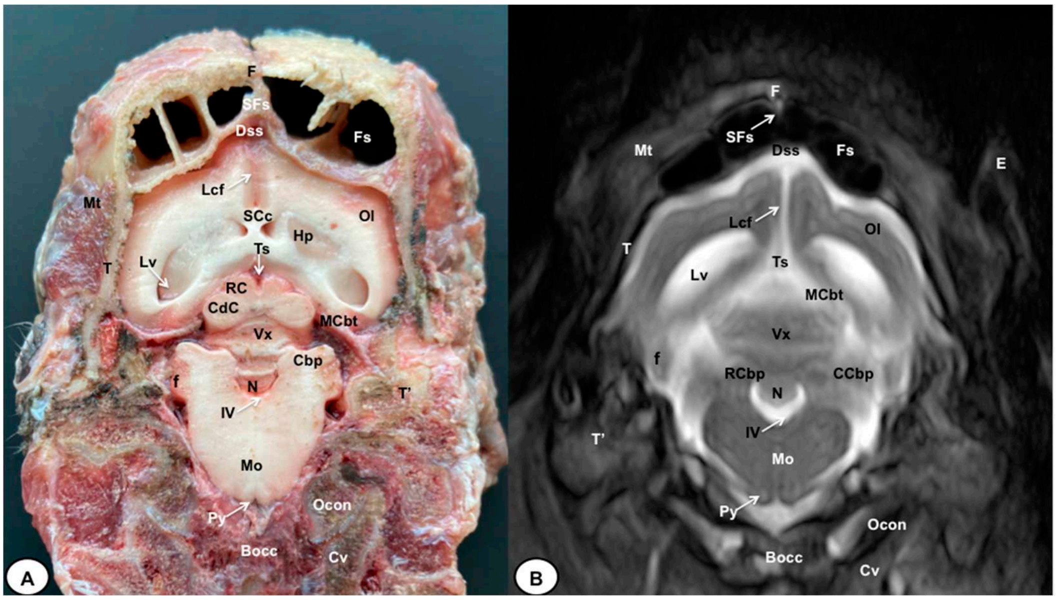

Figure 6. Transverse gross-section (A) and T2W MR (B) images of the crested porcupine head. F: Frontal bone. Fs: Frontal sinuses. SFs: Septum of frontal sinuses. T: Temporal bone squama. Mt: Musculus temporalis. T′: Tympanic and petrous parts of temporal bone. Dss: Dorsal sagital sinus. Lcf: Longitudinal cerebral fissure. Lv. Lateral ventricle. SCc: Splenium of corpus callosum. Hp: Hippocampus. Ts. Transverse sinus. MCbt: Membranous cerebellar tentorium. RC: Rostral colliculus. CdC: Caudal colliculus. Cbp: Cerebellar peduncle. Vx: Vermis of cerebellum. RCbp: Rostral cerebellar peduncle. CCbp: Caudal cerebellar peduncle. N: Nodule. IV: Fourth ventricle. Mo: Medulla oblongata. Py: Pyramids of the medulla oblongata. Cv: First cervical vertebra. Ocon: Occipital condyle. Bocc: Basioccipital bone. E. External ear.

 doi:10.20944/preprints202305.2165.v1

3.2. Magnetic Resonance Imaging (MRI)

No significant anatomic differences were identified subjectively in the two porcupines imaged. Most anatomic structures seen on T2-weighted images of the cadaver specimens matched adequately with structures identified in the corresponding anatomic gross sections. Hence, the **central nervous system** structures of the porcupine head, as well as the **eyeball's structures** (vitreous humour and lens), and the **masticatory muscles,** showed an accurate visualization using T2W MR images. Nonetheless, those bones that comprised the neurocranium, such as the frontal, the parietal, the temporal, the occipital and the sphenoid bones were identified with a hypointense signal (Figs. 2B, 3B, 4B, 5B, 6B, 7A, 7B).

In the transverse planes of the encephalon, identifiable structures of the brain were observed slightly more hyperintense than the white matter, which was more hypointense in T2W sequences (Figs. 3B, 4B, 5B, 6B). Moreover, the two sagittal and dorsal (Figs 7, 8), as well as the different transverse T2W images were useful in depicting the different components that comprise the ventricular system that showed a hyperintense signal. Hence, the lateral ventricles, as well as the dorsal and ventral parts of the third ventricle were displayed (Figs 3B, 4B, 5B, 6B, 7A, 8), and among these, we observe the interthalamic adhesion, limited laterally by the right and left sides of the thalamus (Fig. 7A). Besides, transverse, sagittal and parasagittal T2W images displayed with adequate detail the dorsal and ventral parts of the hippocampus (Figs. 4B, 5B, 7B). In addition, the tectum mesencephali with the caudal colliculus and the fourth ventricle was also displayed with excellent detail (Figs. 7a, 7B). Other essential components of the CNS such as the vermis of the cerebellum with the different lobes observed from above and behind could be distinguished in the sagittal T2W images (Fig. 7A). Hence, the moderate contrast between grey and white matter was helpful to distinguish the different lobes. Thus, the dorsal lobes of the cerebellum (the rostral and ventral culmen, the declive, the folium, the tuber and the pyramid), as well as its ventral lobes (the lingula, the nodulus, and the uvula) were identified. In addition to these findings, we also observed the rostral and caudal cerebellar peduncles (Figs. 6B, 8A). This technique also enables an adequate resolution to identify the muscles involved in the masticatory function and already mentioned in the gross section images.

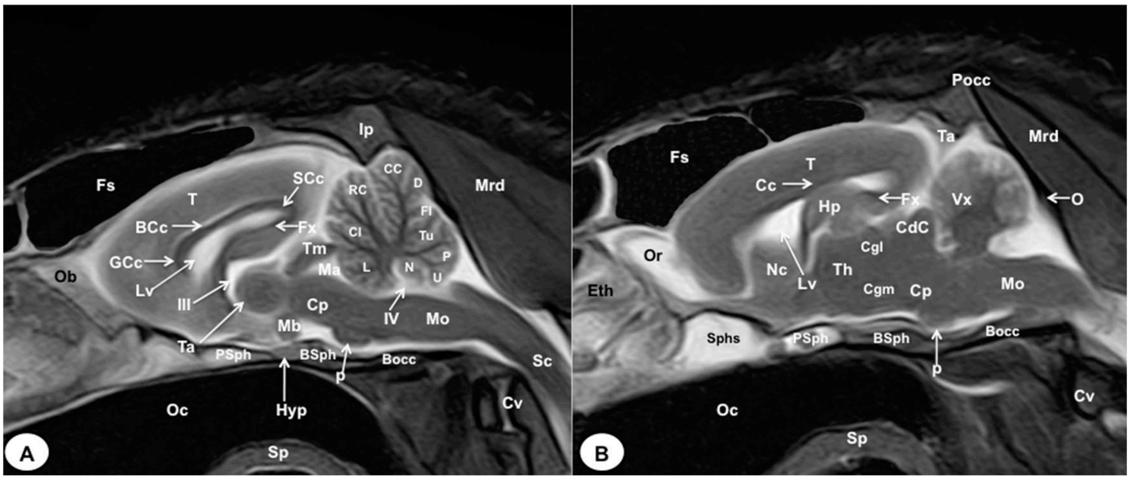

Figure 7. : Sagittal (A) and Parasagittal (B) T2W MR images of the crested porcupine head. Fs: Frontal sinuses. Ip: Interparietal bone. Pocc: *Protuberantia occipitalis externa.* Eth: Ethmoturbinates. Ob: Olfactory bulb. Or: Olfactory recess. T: Telencephalon. Lv. Lateral ventricle. Cc: *Corpus callosum.* GCc: Genu of corpus callosum. BCc: Body of corpus callosum. SCc: Splenium of corpus callosum. Hp: *Hippocampus.* Fx: Fornix. Nc: *Nucleus caudatus.* III: Third ventricle. Ta: Interthalamic adhesion. Th: *Thalamus.* Cgl: *Corpus geniculatum laterale* (lateral geniculate body). Cgm: *Corpus geniculatum mediale* (medial geniculate body). Mb: Mamillary body. Hyp: *Hypophysis.* Ta: Tentorial process. Tm: Tectum of mesencephalon. Ma: Mesencephalic aqueduct. CdC: Caudal colliculus. Cp: Cerebral peduncle. Vx: Vermis of cerebellum. L: Lingula. Cl: Central lobe of cerebellum. RC: Rostral culmen. CC: Caudal culmen. D: Declive. Fl: Folium. Tu: Tuber. P: Pyramid. U: Uvula. N: Nodule. IV: Fourth ventricle. p:

Pons. Mo: *Medulla oblongata*. Sc: Spinal cord. Cv: Cervical vertebra. Mrd: *Musculus rectus dorsalis.* O: Occipital bone. Sphs: Sphenoid sinus. PSph: Presphenoid bone. BSph: Basisphenoid bone. Bocc: Basioccipital bone. Oc: Oral cavity. Sp: Soft palate.

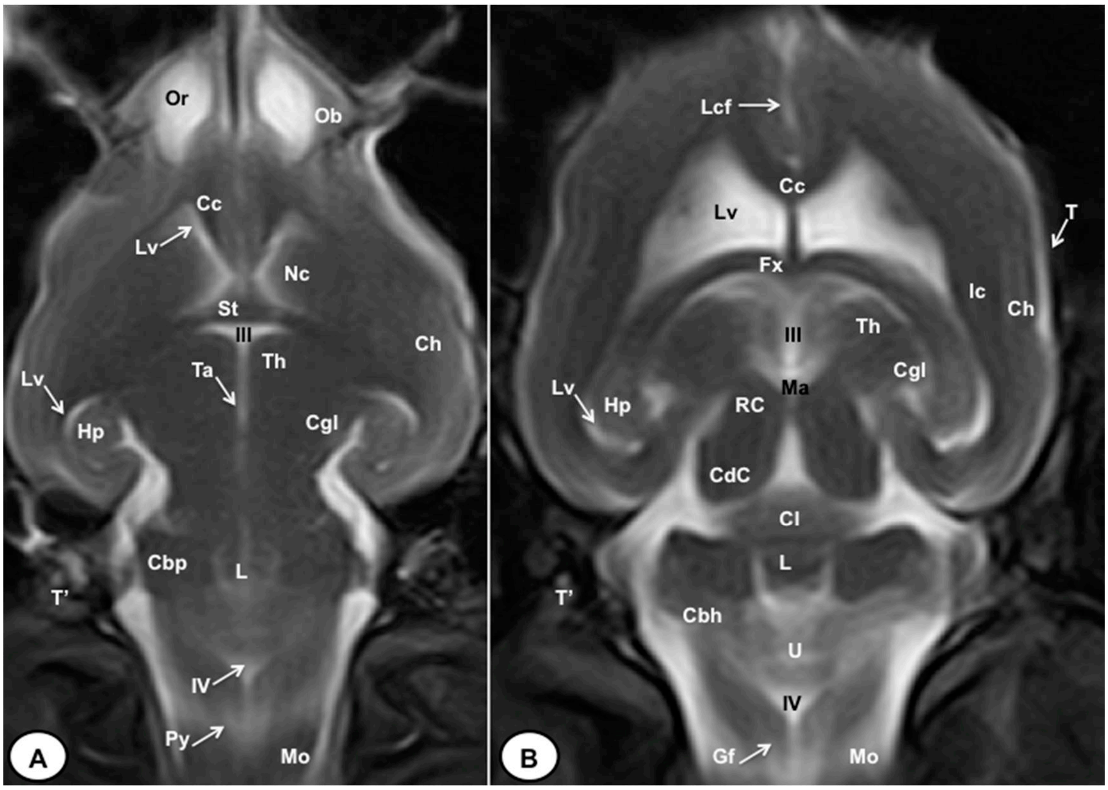

Figure 8. : Dorsal MRI in T2W images of the crested porcupine head at the level of the olfactory bulb (A), and corpus callosum (B). Ob: Olfactory bulb. Or: Olfactory recess. Lcf: Longitudinal cerebral fissure. Cc: Corpus callosum. Lv. Lateral ventricle. Nc: *Nucleus caudatus*. St: *Septum telencephali*. Fx: *Fornix*. III: Third ventricle. Ic: Internal capsule. Ch: Cerebral hemisphere. Hp: *Hippocampus*. Th. *Thalamus*. Ta: Interthalamic adhesion. Cgl: *Corpus geniculatum laterale* (lateral geniculate body). Ma: Mesencephalic aqueduct. RC: Rostral colliculus. CdC: Caudal colliculus. Cl: Central lobe of cerebellum. L: *Lingula*. Cbp: Cerebellar peduncle. Cbh: Cerebellar hemisphere. IV: Fourth ventricle. Mo: *Medulla oblongata*. Py: Pyramids of the medulla oblongata. Gf: Gracile fasciculus. T: Temporal bone squama. T': Tympanic and petrous parts of temporal bone.

4. Discussion

In recent years, modern diagnostic imaging techniques such as computed tomography and magnetic resonance imaging have become quite fashionable in captive and free-ranging animals to diagnose and treat several diseases since their availability for clinical use has dramatically increased. However, the costs and an increased risk of complications due to general anaesthesia [11,12] are limiting factors to the use of these techniques in exotic animals. In contrast with traditional imaging methods such as radiography and ultrasound, which are widespread among veterinarians [10], these procedures can provide images of the different structures in various planes without repositioning the animal [12,16,22,23]. CT provides more anatomic detail about the skull bones and dentition compared to MRI [16]. Nonetheless, some clinical processes affecting rodents can present secondary soft tissue involvement that can be better visualized using MRI. Magnetic resonance imaging is considered the gold standard to image the brain in humans and animals. Besides, MRI permits the identification of structures deep into bone and air and is less limited by operator experience [3,11,12,14]. Therefore, this technique improves anatomic identification and lesion detection allowing assessment, detailed prognosis, diagnosis of underlying lesions and treatment choice [11,12]. Thus, they have been used in different species of rodents to evaluate a variety of head processes that are not well visualized

Preprints (www.preprints.org) | NOT PEER-REVIEWED | Posted: 31 May 2023 doi:10.20944/preprints202305.2165.v1

through standard imaging techniques. Among these, we included dental disease and its associated problems, deformities, and osteomyelitis, as well as the extension of the infection process to different bone cavities of the skull as the nasal or the paranasal cavities, and the tympanic bullae, fractures and neoplasia [10-12]. Nonetheless, these modern imaging techniques have important limitations that must be considered, such as their expense, the use of sedation, and the time demanded for data analysis. Despite these disadvantages, its use in endangered species is justified since the amount of valuable information obtained with little risk to the animal [3,22,23]. In this study, the images obtained by these procedures displayed excellent detail of the CNS and associated structures, providing additional information to the gross-section anatomical images. To the authors' knowledge, this is the first description of the CNS and associated structures of the crested porcupine using gross-section and modern diagnostic imaging techniques such as MRI.

In veterinary practice, the study of nervous structures within the head is arduous because of the anatomic complexity. Therefore, the gross-anatomical sections were quite helpful providing an accurate morphologic characteristic of the crested porcupine CNS and associated structures mainly related to the eyeball and those components of the auditory system. Because of the broad slice interval used in this study, the same structures were not visible on the transverse views. Similar studies in other exotic species such as rabbits, iguanas and loggerhead turtles, have proven that this combination is essential to compare the relative positions and sizes of cephalic and other anatomic structures [3,14,24,25].

The MR images obtained in the transverse and sagittal planes were generated without repositioning the head and with a high-field magnet that facilitated an adequate evaluation of the head of the crested porcupine. Although the transverse images provide detailed anatomical information, the different planes used here did the identification more obvious. In addition, subjective image analysis and objective measurements of the present study also demonstrated a rather large dorsal *metencephalon* concerning a smaller *telencephalon* when compared to dogs of similar size and weight. Müllhaupt et al., (2015) observed similar findings in size when they studied the rabbit brain with a high field-strength magnet. Nonetheless, further studies with a larger number of crested porcupines should be done to confirm this finding.

Moreover, the present study showed that this technique was helpful in visualizating the bone and soft tissue structures of the porcupine head. Thus, excellent discrimination of the main components of the *encephalon*, such as the *rhinencephalon, telencephalon, diencephalon, mesencephalon, metencephalon,* and *myelencephalon* could be distinguished with the T2W images. The T2W images have demonstrated to be useful for anatomical studies in different exotic species [3,12,22-30]. Therefore, transverse MR images T2W showed the olfactory bulb and its recess, which was hyperattenuated compared to the *telencephalon*. Similar enhancement was found in rabbits, especially in the sagittal plane [14,15]. Besides, the sagittal MR T2W images were essential to exhibit the different lobes observed in the vermis of the cerebellum, which displayed a hyperintense/isointense signal when compared with the cerebellar white matter that was hypointense. As mentioned in other studies [24], the use of cadavers did not allow the administration of an intravenous contrast medium, which could provide better resolution of the MR images. This limitation and the low number of specimens should be taken into consideration in further studies performed on this species. Nevertheless, the use of MRI and macroscopic anatomical section provided adequate information for anatomic evaluation in teaching and clinical purposes. In contrast to other studies conducted in rodents and rabbits [15, 29,30], we have used gross sections and done an exhaustive anatomical description, location, and intensity of the different structures that comprise the central nervous system of the crested porcupine. On the other hand, the images obtained in the sagittal plane, in contrast with those displayed in the transverse plane, facilitated a better assessment of the topographic anatomic structures in the median plane, which comprised mainly the intracranial cavity and the central nervous system and associated structures. Similar findings have been reported in other studies performed on exotic species using MRI [3,24]. Hence, all the images obtained in this study can serve as initial reference material to support pathological studies of crested porcupine heads.

5. Conclusions

The combination of modern imaging techniques such as magnetic resonance imaging and anatomical sections used in this study was quite helpful providing essential references of the different bone and soft tissue structures comprising the SNC and sensory organs of the crested porcupine. Therefore, the information obtained in this study was useful to the anatomic and clinical evaluation of numerous pathologic processes involving the head of these animals, such as abscesses, metabolic bone diseases, fractures, inflammation and neoplasia. Besides, the MR images obtained in different spatial planes could facilitate understanding of the anatomic organization for our students since these procedures allow the visualization of structures without overlapping, eliminating the difficulties of visualizing specific anatomic structures. Nevertheless, the high cost and accessibility of this equipment do not facilitate its use on porcupines or rodents in daily veterinary practice.

Author Contributions: Conceptualization, J.R.J., A. E. and M.E.; methodology, J.R.J., D.M. and M.E.; formal analysis, J.R.J., D.M. and M.E.; investigation, J.R.J., A. E., D.M., and M.E.; resources, D.M.; writing—original draft preparation, J.R.J. and D.M.; writing—review and editing, J.R.J., D.M., and M.E. All authors have read and agreed to the published version of the manuscript.

Institutional Review Board Statement: As happens in domestic mammals, just informed consent from the owner, allowed us to carry out this study. Therefore, Rancho Texas Lanzarote Park was informed that all animal identity information obtained from this study was treated as confidential to the extent permitted by law, and only used for research or teaching purposes.

Informed Consent Statement: Informed consent was obtained from all subjects involved in the study.

Acknowledgments: In loving memory of Alvaro Domingo and Honorio Rodriguez Garcia. We also thank Ayesh Mohamad, Carmen Mingot, Marisa Mohamad, and Jamal Jaber for their support and constructive comments, and Rancho Texas Lanzarote Park to provide the animals of this study.

Conflicts of Interest: The authors declare no conflict of interest.

References

1. Banzato T, Russo E, Di Toma A, Palmisano G, Zotti A. Anatomic imaging of the Boa constrictor head: A comparison between radiography, computed tomography and cadaver anatomy. *Am J Vet Res* **2011**; 72: 1592–1599.
2. Van Caelenberg AI, De Rycke LM, Hermans K, et al. Comparison of radiography and CT to identify changes in the skulls of four rabbits with dental disease. *J Vet Dent* **2011**; 28: 172–181.
3. González Rodríguez E, Encinoso Quintana M, Morales Bordon D, Garcés JG, Artiles Nuez H, Jaber JR. Anatomical Description of Rhinoceros Iguana (Cyclura cornuta cornuta) Head by Computed Tomography, Magnetic Resonance Imaging and Gross-Sections. Animals **2023**; 13, 955.
4. Arencibia A, Corbera JA, Ramírez G, Díaz-Bertrana ML, Pitti L, Morales M, Jaber JR. Anatomical Assessment of the Thorax in the Neonatal Foal Using Computed Tomography Angiography, Sectional Anatomy, and Gross Dissections. *Animals* **2020**; 10, 1045.
5. Zafra R, Carrascosa C, Rivero M, Peña S, Fernández T, Suarez-Bonnet A, Jaber JR. Analysis of equine cervical spine using three-dimensional computed tomographic reconstruction. *J Appl Anim Res* **2012**; 40 (2): 108-111.
6. Amori G, De Smet K. "Hystrix cristata". IUCN Red List of Threatened Species. **2016:** e.T10746A22232484.
7. Wilson DE, Reeder DM. eds. "Species Hystrix (Hystrix) cristata". Mammal Species of the World: A Taxonomic and Geographic Reference (3rd ed.) **2005**. Johns Hopkins University Press. p. 1543.
8. Angelici FM, Colangelo P, Gippoliti S. Out of Europe: Investigating Hystrix cristata (Rodentia: Hystricidae) skull morphometric geographic variability in Africa. *Biogeographia* **2021**; 36: a001.
9. Storch G. Porcupines. Pages 300-307 in B. Grzimek, editor. Grzimek1s Encyclopedia of Mammals **1990**. McGraw-Hill, New York.
10. Capello V, Cauduro A. Comparison of diagnostic consistency and diagnostic accuracy between survey radiography and computed tomography of the skull in 30 rabbits with dental disease. *J Exot Pet Med* **2016**; 25 :115–127.
11. Capello V. Diagnostic Imaging of Dental Disease in Pet Rabbits and Rodents. *Vet Clin North Am Exot Anim Pract* **2016;** 19(3):757-82.
12. Glodek J, Adamiak Z, Przeworski A. Magnetic Resonance Imaging of Reptiles, Rodents, and Lagomorphs for Clinical Diagnosis and Animal Research. *Comp Med* **2016**; 66: 216–219.

Preprints (www.preprints.org) | NOT PEER-REVIEWED | Posted: 31 May 2023 doi:10.20944/preprints202305.2165.v1

13. Fornazari F, Guimaraes FF, Teixeira CR, Langoni H. Isolation of staphylococcus epidermidis from inflamed upper respiratory tract of an orange-spined hairy dwarf porcupine (Sphiggurus villosus). *J Venom Anim Toxins Incl Trop Dis* **2012;** 18 (4): 455-458.
14. Van Caelenberg AI, De Rycke LM, Hermans K, Verhaert L, van Bree HJ, Gielen IM. Low-field magnetic resonance imaging and cross-sectional anatomy of the rabbit head. *Vet J* **2011;**188:83–91.
15. Müllhaupt D, Augsburger H, Schwarz A, Fischer G, Kircher P, Hatt JM, Ohlerth S. Magnetic resonance imaging anatomy of the rabbit brain at 3 T. *Acta Vet Scand* **2015**; 28;57(1):47.
16. Capello V, Lennox A. Advanced diagnostic imaging and surgical treatment of an odontogenic retromasseteric abscess in a guinea pig. *J Small Anim Pract* **2015**; 56:134–137.
17. Muñoz-Moreno E, Arbat-Plana A, Batalle D, Soria G, Illa M, Prats-Galino A, Eixarch E, Gratacos E. A magnetic resonance image based atlas of the rabbit brain for automatic parcellation. *PLoS One* **2013;** 8:e67418.
18. Shek JW, Wen GY, Wisniewski HM. Atlas of the rabbit brain and spinal cord. Basel: Karger; **1986.**
19. Popesko P, Rajtova V, Horak J. Anatomy of small laboratory animals. London: Wolfe Publishing Ltd; **1990**. pp. 14–53.
20. Gray-Edwards HL, Salibi N, Josephson EM, Hudson JA, Cox NR, Randle AN, McCurdy VJ, Bradbury AM, Wilson DU, Beyers RJ, Denney TS, Martin DR. High resolution MRI anatomy of the cat brain at 3 Tesla. *J Neurosci Methods* **2014**; 227:10–17.
21. International Committee on Veterinary Gross Anatomical Nomenclature . Nomina anatomica veterinaria. 5. New York: Ithaca; **2012.**
22. Arencibia A, Encinoso M, Jaber JR, Morales D, Blanco D, Artiles A, Vázquez JM. Magnetic resonance imaging study in a normal Bengal tiger (Panthera tigris) stifle joint. *BMC Vet Res* **2015;** 11, 192.
23. Jaber JR, Encinoso M, Morales D, Artiles A, Santana M, Blanco D, Arencibia A. Anatomic study of the normal Bengal tiger (Panthera tigris tigris) brain and associated structures using low field magnetic resonance imaging. *Eur J Anat* **2016**; 20, 195–203.
24. Arencibia A, Hidalgo M, Vázquez JM, Contreras S, Ramírez G, Oros J. Sectional anatomic and magnetic resonante imaging features of the head of juvenile loggerhead sea turtles (Caretta careta). *Am J Vet Res* **2012;** 73: 1119-1127.
25. Valente AL, Cuenca R, Zamora M, Parga M, Lavin S, Alegre F, Marco I. Sectional anatomic and magnetic resonance imaging of coelomic structures of loggerhead sea turtles. *Am J Vet Res* **2006;** 67:1347–1353.
26. Arencibia A, Matos J, Encinoso M, Gil F, Artiles A, Martínez-Gomariz F, Vázquez JM. Computed tomography and magnetic resonance imaging study of a normal tarsal joint in a Bengal tiger (Panthera tigris). *BMC Vet Res* **2019;** 15, 126.
27. Snow TM, Litster AL, Gregory RJ. Big cat scan: Magnetic resonance imaging of the tiger. *Australas Radiol* **2004;** 48, 93–95.
28. Encinoso M, Oros J, Ramírez G, Jaber JR, Artiles A, Arencibia A. Anatomic Study of the Elbow Joint in a Bengal Tiger (Panthera tigris tigris) Using Magnetic Resonance Imaging andGross Dissections. *Animals* **2019;** 9(12):1058.
29. Muñoz-Moreno E, Arbat-Plana A, Batalle D, Soria G, Illa M, Prats-Galino A, Eixarch E, Gratacos E. A Magnetic Resonance Image Based Atlas of the Rabbit Brain for Automatic Parcellation.
30. Chuang N, Mori S, Yamamoto A, Jiang H, Ye X, et al. An MRI-based atlas and database of the developing mouse brain. *NeuroImage* **2011;** 54: 80–89.